



LAWRENCE
LIVERMORE
NATIONAL
LABORATORY

LLNL-TR-686316

Evaluation of the Fluence Conversion Factor for ^{32}P in Sulfur

C. T. Wong

March 18, 2016

Disclaimer

This document was prepared as an account of work sponsored by an agency of the United States government. Neither the United States government nor Lawrence Livermore National Security, LLC, nor any of their employees makes any warranty, expressed or implied, or assumes any legal liability or responsibility for the accuracy, completeness, or usefulness of any information, apparatus, product, or process disclosed, or represents that its use would not infringe privately owned rights. Reference herein to any specific commercial product, process, or service by trade name, trademark, manufacturer, or otherwise does not necessarily constitute or imply its endorsement, recommendation, or favoring by the United States government or Lawrence Livermore National Security, LLC. The views and opinions of authors expressed herein do not necessarily state or reflect those of the United States government or Lawrence Livermore National Security, LLC, and shall not be used for advertising or product endorsement purposes.

This work performed under the auspices of the U.S. Department of Energy by Lawrence Livermore National Laboratory under Contract DE-AC52-07NA27344.

Evaluation of the Fluence Conversion Factor for ^{32}P in Sulfur

When ^{32}S is exposed to neutrons it undergoes a $^{32}\text{S}(\text{n,p})^{32}\text{P}$ reaction with a neutron cross section as shown in Figure 1. This reaction may be used to characterize the neutron fluence for neutrons greater than 3 MeV. The ^{32}P activity is measured and a fluence conversion factor is applied to determine the total neutron fluence above 3 MeV. The fluence conversion factor may be empirically determined by exposing ^{32}S to a characterized neutron flux, or theoretically calculated from the neutron cross section for ^{32}S .

For the LLNL Neutron Activation Dosimeters (NADs) the fluence conversion factor was established by Hankins in 1984. This value was based on measurement of exposed sulfur pellets to a series of three different exposures to a known neutron flux using the Health Physics Research Reactor located at Oak Ridge National Laboratory (personal communication with Hankins). It is believed that the ^{32}P in the sulfur pellets were measured using Beckman Widebeta and Sharp Lowbeta gas-flow proportional counters which are no longer available. The fluence conversion factor (CF_ϕ) for the personnel NAD was empirically determined by comparing the known neutron fluence to the decay corrected activity of ^{32}P in a series of sulfur pellets exposed for three different fluences¹.

$$CF_\phi = \frac{\sum_{i=1}^3 \left(\frac{n/\text{cm}^2}{\mu\text{Ci/g}} \right)_i}{3}$$

Due to the difficulty of preparing a sulfur pellet with a known activity of ^{32}P , the gas flow proportional counters were calibrated using 51 mm electroplated $^{90}\text{Sr}/^{90}\text{Y}$ sources when measuring the Fixed NAD (FNAD) sulfur pellets and a 25 mm $^{90}\text{Sr}/^{90}\text{Y}$ sources when measuring the smaller Personnel NAD (PNAD) sulfur pellets (Hankins Notebook #9 August 1984). The calibration sources used and the efficiencies are provided in Appendix A. Thus the fluence conversion factor incorporates a geometry factor which corrects for the difference in geometry and radionuclide between ^{32}P in the sulfur pellet and the calibration sources.

The above empirically derived fluence conversion factor is problematic in that it is dependent on the counting geometry. The activity of the ^{32}P in the sulfur pellet is unknown (activity results are relative to the calibration sources). If the sulfur pellet is counted in a different geometry, *i.e.* crushed, a different fluence conversion factor is required. Also, this method does not allow for inter-comparisons of ^{32}P in sulfur and fluence conversion factors.

A discussion on the fluence conversion factors used for sulfur is included in the *LLNL Nuclear Criticality Accident System – Technical Basis*². The historical fluence conversion factors used are summarized in Table 1.

¹ The Fixed NAD value was also determined using exposures to the same three fluences.

² Lawrence Livermore National Laboratory's Nuclear Criticality Accident System, Technical Basis, September 2012.

Table 1 - Historical Fluence Conversion Factors for Sulfur

	Geometry	Geometry Factor	Personnel NAD CF_φ³	Fixed NAD CF_φ⁴
Hankins, 1984	Whole Pellet		2.9E+13	1.2E+13
1991	Crushed Pellet	4.9	5.9E+12	
2003	Crushed Pellet	3.8	7.7E+12	
2010	Crushed Pellet	3.0	2.0E+12	

“The decay corrected activity concentration (i.e., activity per gram) for each element in the LLNL design is converted to fluence using factors established by Hankins (Hankins, 1984). The fluence to activity conversion factor for the sulfur pellet measurement was originally established by Hankins to be $2.9 \times 10^{13} \left(\frac{n/cm^2}{\mu Ci/g} \right)$ (Hankins, 1984). A change in the activity to the fluence conversion value for sulfur originally established by Hankins was made in approximately 1991. The change in the fluence conversion value represented a change in the method used to measure the sulfur. When removed from the LLNL holder the sulfur pellet was typically found to be in several pieces. Consequently it was decided to grind the sulfur and spread the powder evenly within a counting planchet rather than attempting to count the intact pellet as was done by Hankins. The fluence conversion factor for the sulfur was modified in 1991 to reflect a change in counting geometry. The modifying factor was determined by counting a whole pellet and then counting the pellet after it was ground into powder. The ratio of efficiency for ground sulfur versus the pelletized sulfur was determined to be 4.9, thus changing the original Hankins derived fluence conversion value of 2.9×10^{13} to $5.9 \times 10^{12} \left(\frac{n/cm^2}{\mu Ci/g} \right)$. In approximately 2003, testing indicated that the 4.9 ratio was approximately 30% high resulting in a new fluence conversion value of $7.7 \times 10^{12} \left(\frac{n/cm^2}{\mu Ci/g} \right)$. Whole pellet versus crushed pellet evaluations in September 2010 measured ratios of the whole pellet to crushed pellet to be 3.0 using current beta counting equipment, thus suggesting a fluence conversion value of $2.0 \times 10^{12} \left(\frac{n/cm^2}{\mu Ci/g} \right)$. Additional testing and data is needed to better explain observed differences in the whole to crushed pellet ratio. Based on Hankins’ original work, and the 2003 and 2010 evaluations, if the whole pellet is measured (without any breaks in the pellet) the fluence conversion factor of $2.9 \times 10^{13} \left(\frac{n/cm^2}{\mu Ci/g} \right)$ should be used, and if ground sulfur powder is measured a fluence conversion factor of $5.9 \times 10^{12} \left(\frac{n/cm^2}{\mu Ci/g} \right)$ should be used.”

³ Using 25mm Calibration source.

⁴ Fixed NAD factor added from Hankins 1988 UCRL-50007-88

Recent Exposures.

Between 2009 and 2014 several inter-comparison and characterization experiments were done at various reactors (2009 Silene, 2010 CALIBAN⁵, 2013 Flat Top and 2014 Godiva). These experiments allowed us to re-visit the processes involved in measurement of the sulfur pellets. For the 2009 Silene experiments, portable Ludlum 3030 swipe counters with Ludlum 43-10-1 scalers were used. Subsequent to the Silene experiments a Canberra iSolo 300G radon-compensating alpha/beta counter was purchased for the measurements. For the 2010 CALIBAN experiments, the iSolo was calibrated with a source similar in geometry to those used for the historical and Silene experiments. The calibration source was a 50 mm electroplated ⁹⁰Sr/⁹⁰Y standard mounted at the bottom of a stainless steel planchet (Figure 2). For the 2013 Flat Top and 2014 Godiva experiments, 50 mm ⁹⁰Sr/⁹⁰Y sources, purchased for use with the iSolos (Figure 3), were mounted in a carrier placing the sources closer to the detector than previous experiments. Summaries of the detector information are provided in Appendix A.

During the 2009 Silene experiments 24 sulfur pellets were exposed during three experiments. The pellets were counted as whole pellets (Figure 4) on the Ludlum swipe counters, then crushed, transferred to a stainless steel planchet, and covered with mylar (0.25 mil) for counting (Figure 5).

For the 2010 CALIBAN experiments 27 PNADs and 16 FNADs were exposed to two pulse irradiations. The sulfur pellets were counted as whole pellets in both face-up (pellet facing the reactor) and face-down (pellet facing away from the reactor) geometries. No significant difference in count rates for the pellets counted face-up versus the pellets counted face-down was observed. For this experiment the samples were not crushed as it was observed during the 2009 Silene experiments that crushing the pellets added variability to the analysis results.

For the 2013 Flat Top experiments, four PNADs and three FNADs were exposed. The pellets were counted as a whole pellet, then gently crushed, transferred to a stainless steel planchet, and melted into a disk for counting (Figure 6).

For the 2014 Godiva experiment 144 PNADs and 15 FNADs were exposed to three separate bursts at 250 degrees, 140 degrees and 70 degrees. The whole pellets were counted on iSolo counters. These pellets were then shipped back to LLNL for additional measurements.

⁵ D.P. Hickman, A.R. Wysong, D.P. Heinrichs, C.T. Wong, M.J. Merritt, J.D. Topper, F.A. Gressmann, D. J. Madden, Evaluation of LLNL's Nuclear Accident Dosimeters at the CALIBAN Reactor, September 2010.

Counting Geometry.

Throughout these experiments efforts were made to determine an optimum counting geometry for the sulfur pellets. Once an optimum counting geometry was determined, experiments could be performed to determine the counting efficiency for that geometry. Table 2 provides a summary of the advantages and disadvantages of the proposed counting geometries.

Table 2- Comparison of Counting Geometries

Geometry	Advantages	Disadvantages
Whole Pellet	<ul style="list-style-type: none">- Consistent geometry- No preparation required	<ul style="list-style-type: none">- Count rate appears to increase if the pellet is broken- Low efficiency due to attenuation- Efficiency unknown
Crushed Pellet	<ul style="list-style-type: none">- Increased counting efficiency	<ul style="list-style-type: none">- Effort required to crush the pellets- Potential for loss of material and cross-contamination- Inconsistent counting geometry- Efficiency may be dependent on how fine the powder is crushed- Efficiency unknown
Melted Pellet	<ul style="list-style-type: none">- Consistent geometry- Increased counting efficiency compared to whole pellet	<ul style="list-style-type: none">- Effort required to crush and melt the pellet- Potential for loss of material and cross-contamination

Experiments performed at LLNL subsequent to the 2014 Godiva runs demonstrate that there is a small but insignificant increase (activity ratio whole/broken = 1.06 ± 0.05) in the count rate for pellets which are broken into two pieces (Appendix B). Since it is expected that only a small percentage of the pellets will be broken, this small increase in activity is negligible in determining the overall neutron fluence.

For future measurements, the simplicity of counting the sulfur as a whole pellets, and the consistency of the count rates, outweighs the disadvantage of the lower counting efficiency due to attenuation. Further experiments described in this document provide an estimate of the counting efficiency for the sulfur pellet.

Comparisons Between Detection Systems.

Although the iSolo counters have been used for these experiments since 2010, for a criticality event that occurs at LLNL, the samples may be counted on various other detectors available at LLNL. Selected sulfur pellets from the 2014 Godiva experiments (68) were counted on the various detectors as whole pellets and as crushed pellets. Additionally sixteen samples were counted as melts. A summary of this data is provided in Appendix C.

As expected for measurements of the pellet on different detectors, as long as the detectors were calibrated similarly the activity concentrations are comparable.

Activity Ratio of Whole Pellet vs. Crushed Pellet vs. Melt.

The fluence conversion factor for sulfur was changed several times due to different measurements of the ratio of activity in the crushed pellet to the activity of the whole pellet. This led to performing additional experiments to characterize this ratio. Appendix D describes the studies performed. From this data and the historical information, it is apparent that there is a wide range of values for the ratio. Although the cause of the variation is unknown, it could be attributed to the method for crushing the pellets (a finer powder would have a higher count rate).

Unlike the measurements of the crushed powder, the activity ratio for the melt to the whole pellet appears to be very consistent. This indicates that the variability in the counting geometry is reduced by preparing the sample as a melt as opposed to crushing the samples.

Counting Efficiency for the Pellet, Eff_{pellet} .

In 2013 a technique was developed which creates a consistent geometry in the form of a melt. The sulfur pellet is gently crushed, transferred as an inverted cone to the center of a ringed stainless steel planchet, then melted on a hot plate (~140 °C) to form a uniform melt (Figure 6). This technique was used to spike the sulfur with a known amount of $^{90}\text{Sr}/^{90}\text{Y}$. The spiked sulfur disk was used to determine the efficiency for the melt geometry, Eff_{melt} . Assuming the efficiency for counting ^{32}P in sulfur is the same as $^{90}\text{Sr}/^{90}\text{Y}$ in sulfur, and given the activity ratio of the pellet to the activity ratio of the melt, one can calculate the efficiency for the pellet, Eff_{pellet} .

$$Eff_{\text{pellet}} = \frac{CPM_{\text{pellet}}}{DPM_{\text{pellet}}} \quad (1)$$

$$CPM_{\text{pellet}} = (uCi/g)_{\text{pellet}}(2.22 \times 10^6)(mass_{\text{pellet}, g})(Eff_{50mm}) \quad (2)$$

$$DPM_{\text{pellet}} = (uCi/g)_{\text{melt}}(2.22 \times 10^6)(mass_{\text{melt}, g})(Eff_{50mm})/Eff_{\text{melt}} \quad (3)$$

$$Eff_{\text{pellet}} = \frac{(uCi/g)_{\text{pellet}}(2.22 \times 10^6)(mass_{\text{pellet}, g})(Eff_{50mm})}{(uCi/g)_{\text{melt}}(2.22 \times 10^6)(mass_{\text{melt}, g})(Eff_{50mm})/Eff_{\text{melt}}} \quad (4)$$

$$mass_{\text{pellet}} = mass_{\text{melt}} \quad (5)$$

$$Eff_{\text{pellet}} = \frac{(uCi/g)_{\text{pellet}}}{(uCi/g)_{\text{melt}}}(Eff_{\text{melt}}) \quad (6)$$

$$Eff_{\text{pellet}} = (Eff_{\text{melt}}) / \frac{(uCi/g)_{\text{melt}}}{(uCi/g)_{\text{pellet}}} \quad (7)$$

This technique was applied to sulfur pellets from the 2013 Flat Top and the 2014 Godiva experiments (Appendix E) yielding the following for the Eff_{pellet} .

Table 3 - 2013 Flat Top Counting Efficiency for the Pellet, Eff_{pellet}

Detector	Detector Type	$\frac{(uCi/g)_{melt}}{(uCi/g)_{pellet}}$	Eff_{melt}	Eff_{pellet}
iSolo (LLNL)	PIPS	2.30 ± 0.21	19.60%	8.52 %

Table 4 – 2014 Godiva Counting Efficiency for the Pellet, Eff_{pellet}

Detector	Detector Type	$\frac{(uCi/g)_{melt}}{(uCi/g)_{pellet}}$	Eff_{melt}	Eff_{pellet}
iSolo (LLNL)	PIPS	2.29 ± 0.10	19.60%	8.56 ± 0.39 %
iMatic (CTRP)	PIPS	2.11 ± 0.07		±
Protean	GPC	2.22 ± 0.09	26.53%	11.94 ± 0.49 %
Tennelec (CTRB)	GPC	2.20 ± 0.10		±

Revised Fluence Conversion Factor.

The current CF_φ incorporates a geometry factor which corrects for the difference in efficiency for the pellet (Eff_{pellet}) and the efficiency of the calibration standard (Eff_{50mm}). In the experiments described in this document the Eff_{pellet} was determined, thus the geometry factor may be removed from CF_φ by multiplying CF_φ by the ratio of the Eff_{pellet}/Eff_{50mm}.

Table 5 – 2013 Flat Top Revised Fluence Conversion Factor, CF_φ

Detector	Detector Type	Eff_{50mm}	Eff_{pellet}	CF_φ
iSolo (LLNL)	PIPS	31.97%	8.58%	0.78x10 ⁻¹²

Table 6 – 2014 Godiva Revised Fluence Conversion Factor, CF_φ

Detector	Detector Type	Eff_{50mm}	Eff_{pellet}	CF_φ
iSolo (LLNL)	PIPS	31.44%	8.56%	0.79x10 ⁻¹²
iMatic (CTRP)	PIPS	36.53%		
Protean	GPC	40.17%	11.97%	0.86 x 10 ⁻¹²
Tennelec (CTRB)	GPC	36.54%		

Appendix A - Detector Information

Historical

Detector¹	Calibration Source	Eff_{51mm}
Counter B ²	51 mm	37.56%
Counter F ³	51 mm	29.44%
Counter F ³	25 mm	29.35%

1. Hankins Notebook #9 August 1984
2. Beckman Widebeta with 5" gas-flow proportional counter
3. Sharp Lowbeta with a 2" gas-flow proportional counter

Manual Counter

Detector¹	Calibration Source²	Eff_{50mm}
Detector 1	CF-264	26.08%
Detector 2	CF-260	28.51%
Detector 3	CF-262	28.00%
Detector 4	CF-253	26.61%
Average		27.32%

1. Manual 2" gas-flow proportional counters, custom built using Canberra modules.
2. 50 mm electroplated ⁹⁰Sr/⁹⁰Y source mounted at the bottom of a stainless steel planchet

Protean MDC-4

Detector¹	Calibration Source²	Eff_{50mm}
MPC A	CF-264	40.50%
MPC B	CF-260	39.63%
MPC C	CF-262	40.95%
MPC D	CF-253	39.61%
Average		40.17%

1. Manual 2" gas-flow proportional counters
2. 50 mm electroplated ⁹⁰Sr/⁹⁰Y source mounted at the bottom of a stainless steel planchet

2009 Silene

Scaler ID¹	Detector ID¹	Voltage	Calibration Source²	Eff_{50mm}	CPM_{BKG}
7002467	PR153450	780 V	CF-251	39.8%	26.7
7002466	PR153449	710 V	CF-251	37.1%	23.5
7002466	PR107402	710 V	CF-251	34.6%	24.3

1. Portable Ludlum 3030 swipe counter with Ludlum 43-10-1 scalars
2. 50 mm electroplated ⁹⁰Sr/⁹⁰Y source mounted at the bottom of a stainless steel planchet

2010 CALIBAN

Detector¹	Detector Type	Calibration Source²	Eff_{50mm}³	CPM_{BKG}³
iSolo #01	PIPS	CF-151	25.35%	17.63
iSolo #02	PIPS	CF-151	26.15%	19.13

1. Canberra iSolo-300G Radon Compensating Alpha/Beta counter
2. 50 mm electroplated ⁹⁰Sr/⁹⁰Y source mounted at the bottom of a stainless steel planchet
3. Average of efficiencies and backgrounds during the period the iSolos were in use

2013 Flat Top

Detector¹	Detector Type	Calibration Source²	Eff_{50mm}	CPM_{BKG}
iSolo	PIPS	MP-154	32.55%	19.00

1. Canberra iSolo-300G Radon Compensating Alpha/Beta counter
2. 50 mm electroplated ⁹⁰Sr/⁹⁰Y source mounted near the detector

2014 Godiva

Detector¹	Detector Type	Calibration Source²	Eff_{50mm}²	CPM_{BKG}
iSolo 4161	PIPS	SZ298	30.99%	10.14
iSolo 28024	PIPS	AB-8984	32.08%	13.48
I solo 60183	PIPS	SZ298	31.71%	15.20

1. Canberra iSolo-300G Radon Compensating Alpha/Beta counter
2. 50 mm electroplated ⁹⁰Sr/⁹⁰Y source mounted near the detector.

Appendix B - Comparison of Broken Pellets to Whole Pellets

Subsequent to the experiments at the Godiva reactor in May 2014, 68 of the sulfur pellets were counted as whole pellets and as melts on various available alpha/beta counters. The results from these measurements are summarized in Table 7.

Table 7 - 2014 Godiva Geometry Factors

Detector	Detector Type	Broken/Whole
iSolo (LLNL)	PIPS	1.06 ± 0.07
iMatic (CTRP)	PIPS	1.05 ± 0.04
Protean	GPC	1.06 ± 0.05
Tennelec (CTRB)	GBC	1.06 ± 0.04
Average		1.06 ± 0.05

Appendix C - Comparisons Between Detection Systems.

The sulfur pellets from the 2014 Godiva experiments were returned to LLNL where selected samples (16) were counted on various counters described in Table 8 below. The samples were then crushed and the powder melted into a disk for counting.

Table 8 - Ratio Compared to the iSolo.

Detector	Detector Type	Eff_{50mm}¹	Pellet	Melt	Melt/Pellet
iSolo	PIPS	30.99%	5.86E-04	1.32E-03	2.25
iMatic (CTRP)	PIPS	36.53%	5.92E-04	1.25E-03	2.11
Protean	GPC	40.17% ²	5.59E-04	1.24E-03	2.21
Tennelec (CTRB)	GPC	36.54% ²	5.89E-04	1.29E-03	2.19
Average			5.82E-04	1.28E-03	2.19

1. Where multiple detectors are used for the same type of instrument the average efficiency for all the detectors used is reported.
2. These sources are mounted at the bottom of a planchet and the distance from the source to the detector is greater than for the sources used to calibrate the iSolos.

Appendix D – Recent Results for Activity Ratio of Whole Pellet vs. Crushed Pellet vs. Melt.

Subsequent to the measurements performed at CALIBAN in September 2010, the sulfur pellets were returned to LLNL for additional measurements. The pellets were used to determine the geometry factor for the crushed pellet to the whole pellet, and a melt to the whole pellet. A Protean low-background gas-flow proportional counter (MPC) was used to count the pellets: a) as a whole pellet, b) as a melt, and c) crushed (only 6 FNADs were crushed). Table 9 summarizes the findings.

Table 9 - 2010 CALIBAN Geometry Factors

	Crushed/Pellet	Melted/Pellet
PNAD	1.50 ± 0.10	1.54 ± 0.12
FNAD	1.32 ± 0.08	2.31 ± 0.07

1. The Geometry Factor is the ratio of the CPM for the sulfur as measured (e.g. crushed, melted) divided by the CPM for the sulfur pellet.

The sulfur pellets exposed during the experiments using the Flat Top reactor in April 2013 were counted on an iSolo detector as whole pellets and as melts. The activity ratio for the melted samples to the whole pellets is given in Table 10.

Table 10 - 2013 Flat Top Geometry Factors

	Melted/Pellet
PNAD	2.30 ± 0.21

Subsequent to the experiments at the Godiva reactor in May 2014, 16 of the sulfur pellets were counted as whole pellets and as melts on various available alpha/beta counters. The results from these measurements are summarized in Table 11.

Table 11 - 2014 Godiva Geometry Factors

Detector	Detector Type	Melted/Pellet
iSolo (LLNL)	PIPS	2.29 ± 0.10
iMatic (CTRP)	PIPS	2.11 ± 0.07
Protean	GPC	2.22 ± 0.09
Tennelec (CTRB)	GPC	2.20 ± 0.10
Average		2.20 ± 0.05

Appendix E - Counting Efficiency for the Pellet, $\text{Eff}_{\text{pellet}}$

As described in the main text, two values are required to determine the efficiency of the pellet, $\text{Eff}_{\text{pellet}}$: 1) the efficiency of the melt (Eff_{melt}); and 2) the ratio of the activity of the melt to the activity of the pellet (equation 7).

The efficiency of the melt was determined by placing measuring a mass of sulfur powder equal to the mass of the sulfur pellet, transferring it to an inverted cone onto the center of a ringed stainless steel planchet, and carefully melting the sample to create a uniform pool of liquid in the center of the planchet (Figure 6). A known activity of a $^{90}\text{Sr}/^{90}\text{Y}$ standard solution was carefully added to the pool of liquid in the planchet. The planchet was allowed to cool, which solidifies the liquid. The solidified disk was counted on an alpha/beta counter (iSolo). The disk was then crushed to homogenize the sample, returned to the planchet and re-melted as described above. The homogenization process was continued until a consistent count rate was obtained. The count rate was used to determine the efficiency of the melt, Eff_{melt} . Three samples were prepared and the average efficiency for the three samples determined.

To determine the ratio of the activity of the pellet to the activity of the melt, four samples from the 2013 Flat Top experiments were counted as whole pellets and as a melt on the iSolo. Also 16 samples from the 2014 Godiva experiments were counted as whole pellets and as a melt on various available detectors. The ratios of the activity of the pellet to the activity of the melt are provided in Appendix C.

Figure 1 – Neutron cross section for S-32(n,p) reaction.

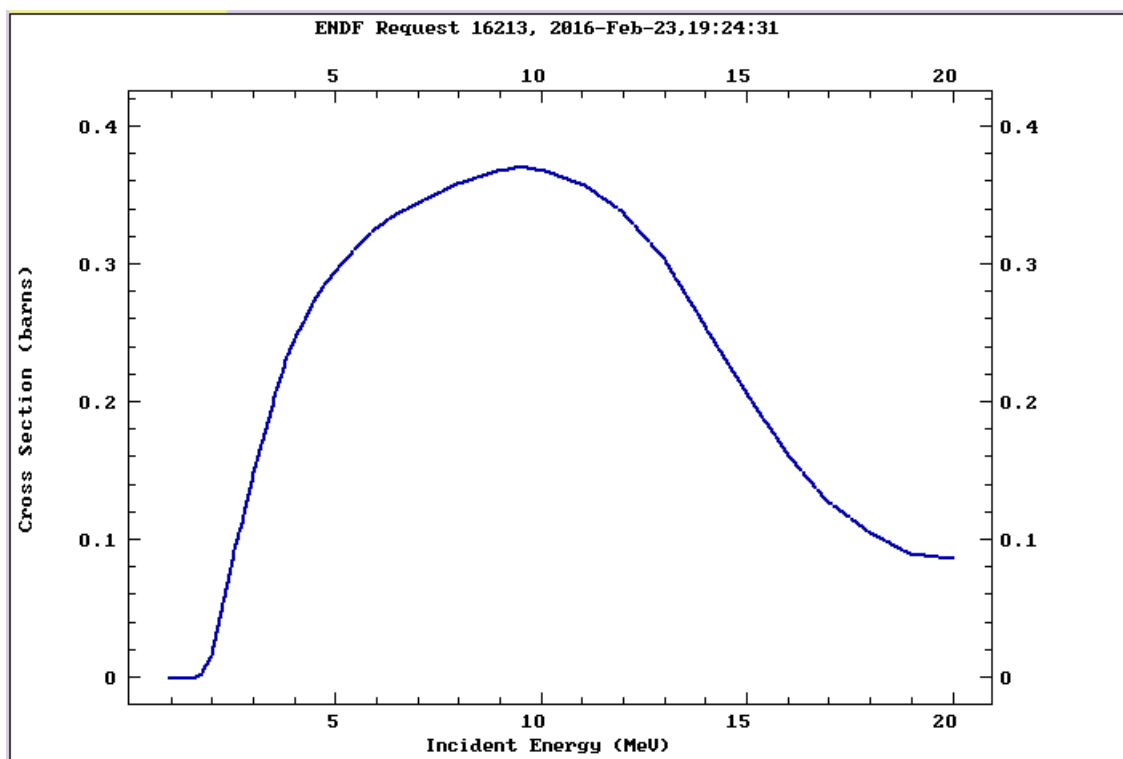


Figure 2 - 50 mm $^{90}\text{Sr}/^{90}\text{Y}$ source mounted at bottom of planchet.



Figure 3 - 50 mm $^{90}\text{Sr}/^{90}\text{Y}$ iSolo source.



Figure 4 - Sulfur Pellet.



Figure 5 - Crushed pellet covered with mylar.



Figure 6 - Melted pellet.

